# Characterization of single magnetic particles with InAs quantum-well Hall devices

G. Landry, M. M. Miller,[a] B. R. Bennett, and M. Johnson
*Naval Research Laboratory, Washington, DC 20375*

V. Smolyaninova
*Department of Physics, Astronomy and Geosciences, Towson University, Towson, Maryland 21252*

(Received 1 June 2004; accepted 27 September 2004)

We have measured the magnetic dipolar field from individual micron-sized spherical ferromagnetic particles. The particles were positioned using an atomic force microscope and measured using submicron Hall sensors fabricated from an InAs single-quantum-well heterostructure with lateral dimensions of 0.5–2.5 $\mu$m. The magnetic moment of individual particles has been measured, verifying their dipolar moment. We also demonstrate a scaling rule for the detection of individual particles which is relevant to the design of biosensors. © *2004 American Institute of Physics*. [DOI: 10.1063/1.1827328]

During the past decade, biosensing that utilized magnetic micro- and nano-particles as labels of specific biomolecular interactions has proven to be a particularly fruitful area of research. Magnetic labels offer advantages over other types of labels such as radioisotopes or fluorophores because the magnetic moment of such a particle not only provides the source of a detectable signal, a localized magnetic field, it also enables the application of controlled forces using external magnetic field gradients. Integrated, microfabricated magnetic field sensors are capable of detecting these magnetic labels and permit arraying. In the future, adaptation of magnetic random access memory may lead to the realization of massive (~1000+analyte) arrays[1] and a particular route using ring shaped elements has been described.[2] Presently, however, the most advanced of these approaches has utilized giant magnetoresistance sensor arrays,[3] but Hall sensors also have been proposed.[4]

The use of magnetic beads as labels in biosensing applications requires detailed knowledge of the magnetic properties of the beads, an understanding of the sensor detection threshold as a function of bead size, and the ability to scale the bead/sensor system to submicron length scales as will be needed for future biosensing applications. This letter presents a systematic study of the characteristics of magnetic beads using Hall sensors in order to address these issues.

The Hall coefficient and noise characteristics of a material depend on the carrier mobility $\mu$ and the inverse of carrier density, $1/n$. It is therefore important to choose a material, such as a quantum well heterostructure, that can provide the necessary characteristics. For this study, the Hall sensors were fabricated from a single quantum well heterostructure: GaAs (substrate) /GaAs–AlSb buffer layer /300 $Al_{0.6}Ga_{0.4}Sb$/15 InAs/12.5 $Al_{0.6}Ga_{0.4}Sb$/5 $In_{0.6}Al_{0.4}As$ /3 InAs/80 sputtered $SiN_x$ (the thickness units are in nanometers). The two-dimensional electron gas (2DEG), at the 15 nm InAs layer, is not intentionally doped but rather the conduction electrons originate, in part, in the InAlAs layer.[5,6] The room temperature mobility and density were $\mu = 21\,600\ \mathrm{cm^2/Vs}$ and $n = 1.2\times10^{12}/\mathrm{cm^2}$ before lithographic processing.

The Hall sensors are defined as a cross shape with an arm width, $w$, of roughly 1 $\mu$m by photolithography and dry etch with an argon ion mill. Some crosses are further defined, with focused ion beam milling, to have arm widths of 500, 600, and 700 nm. Each sensor is characterized using van der Pauw and Hall measurements. After processing, values of the Hall coefficient and sheet resistance were in the range $0.031 < R_H < 0.046\ \Omega/\mathrm{Oe}$ and $150 < R_\square < 600\ \Omega\square/$, respectively.

The experimental method is described with the aid of Fig. 1. Individual magnetic beads are attached to an atomic force microscopy (AFM) cantilever and scanned over the sensor.[2] This permits precise control of both the lateral and vertical position of the bead with respect to the Hall sensor. It also enables simultaneous topographic and Hall voltage imaging, although the large radius of curvature (~2 $\mu$m) of the bead results in fairly crude topographic images. The magnetic beads are a $Fe_{70}Ni_{30}$ nanocomposite with a radius, $a$, of approximately 2 $\mu$m. Magnetization measurements of a dilute ensemble of beads has shown them to be magnetically soft, exhibit negligible remanence, and have a linear magnetization curve at low fields.[7] Because these beads have virtually no remanence, detection requires application of an external magnetic field, $H$, so that the bead develops a magnetic moment $m \propto H$.

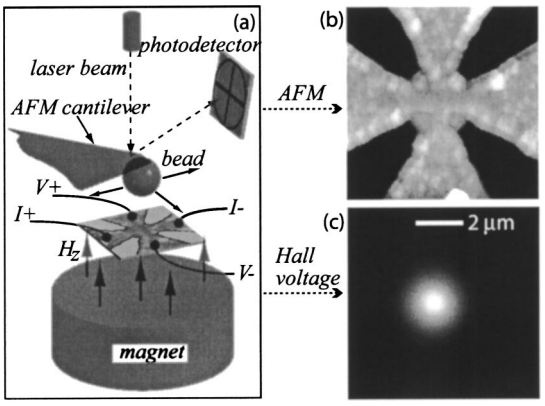


FIG. 1. (a) Measurement setup for Hall sensors in AFM. (b) Topographical image of Hall sensor taken with magnetic bead. (c) Intensity plot of Hall voltage $V_H$, recorded simultaneously with (b).

[a]Electronic mail: michael.miller@nrl.navy.mil

 

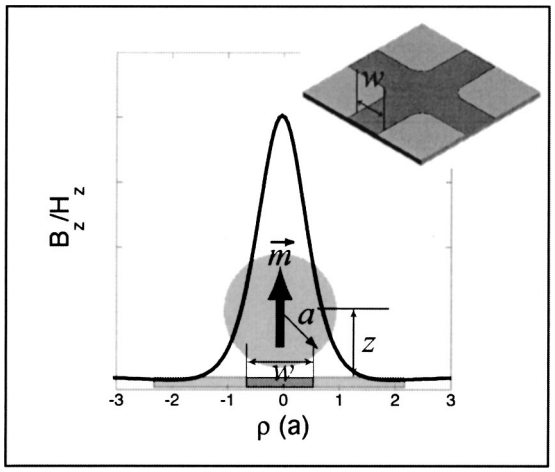


FIG. 2. Normalized field profile $B_z/H_z$ from a magnetized bead with a magnetic moment $\boldsymbol{m}=m\hat{z}$ over a Hall sensor with width $w$. Here $\rho$ is the *radial* distance from the center point under the bead and is given in units of the bead radius $a$. $z$ is the distance from the center of the bead to the quantum well.

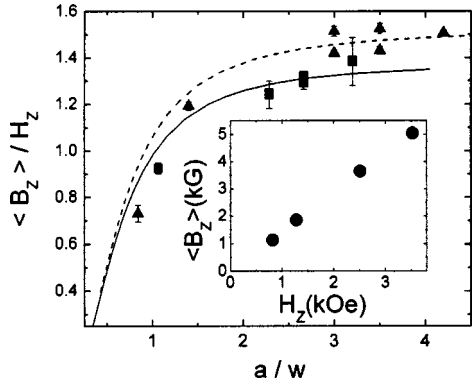


FIG. 3. Magnetic field of $Fe_{70}Ni_{30}$ beads measured with Hall sensors. Data points are the measured bead field normalized to the external field for the 2.1 $\mu$m (triangle) and 1.6 $\mu$m (square) bead. The $x$ axis is the bead radius divided by the nominal Hall sensor dimension. Solid and dashed lines are fits to Eq. (2) for 1.6 and 2.1 $\mu$m beads, respectively, with 0.2 $\mu$m of passivation. The inset shows $\langle B_z\rangle$ vs. $H_z$ for the 2.1 $\mu$m bead measured with a 0.6 $\mu$m Hall cross.

The Hall sensor is placed at the center of the face of a cylindrical magnet that consists of a NdFeB core that is configured with soft-magnetic pole pieces in order to yield a number of discrete magnetic field values, up to 4000 Oe, normal to the face of the magnet. An ac current source provides a bias of $2-5$ $\mu$A at 337 Hz and the Hall sensor output voltage $V_H$ is measured with a lock-in amplifier.

The signal from the lock-in amplifier is fed into an auxiliary AFM data channel so that the Hall voltage is recorded in registry with the topographical signal.[2] These data are shown in Figs. 1(b) and 1(c), respectively. The background magnetic field may be subtracted by moving the bead a sufficient distance ($\sim 5$ $\mu$m) away from the sensor so that the Hall sensor only detects the external field $H=H_z$.

The Hall sensor measures the field of the bead *averaged* over an *effective* area of the Hall sensor. A numerical study of diffusive transport in a 2DEG Hall cross showed that this area can be twice the geometric area.[8] The field from a soft magnetic sphere is expected to be identical to the field from a point dipole having the same moment, located at the center of the sphere.[9] The normal component $B_z$ of this dipolar field is given by

$$B_z(z,\rho)=\frac{m(2z^2-\rho^2)}{(z^2+\rho^2)^{5/2}}, \tag{1}$$

where $m=Ha^3$ is the magnetic moment of the bead, $z$ is measured from the plane of the Hall carriers, and $\rho$ is a transverse dimension, $\rho^2=x^2+y^2$ (refer to Fig. 2), relative to the center of the cross.

When a bead is at position $(x,y,z)$, the perpendicular component $B_z$ has a gradient of values across the area of the sensor and the Hall output voltage is a response to the average value of this field. To calculate the average field $\langle B_z\rangle$ that corresponds to the Hall output voltage $V_H=R_H\times\langle B_z\rangle$, $B_z(z,\rho)$ is integrated over the area of the Hall sensor. We use the approximate geometric area $w^2$ because the effective area is not precisely defined,

$$\langle B_z\rangle=\frac{16Ha^3(w^2/2+z^2)^{1/2}}{w^4+6w^2z^2+8z^4}. \tag{2}$$

The field of a bead is determined by rastering the bead across the Hall cross to get $V_H$, and taking $\langle B_z\rangle=V_H/R_H$. The distance $z$ from the center of the bead to the quantum well, $z=a+t$, includes the bead radius $a$ and a free fitting parameter $t$. The latter includes the thickness of the top barrier of the quantum well and the passivation layer, about 110 nm, plus additional spacing that may arise from a bead asperity or residue on the device and/or bead surface.

We have measured the field from a 1.6 and a 2.1 $\mu$m radius bead using Hall sensors with arm widths ranging from 500 nm to 2.5 $\mu$m and have plotted these data in Fig. 3. The dimensionless units of the $x$ axis are $a/w$, and the $y$ axis is plotted as $\langle B_z\rangle/H_z$. Since we have measured the magnetization of the bead to be linearly proportional to the external field (inset in Fig. 3), $\langle B_z\rangle/H_z$ is constant for a given value of $a/w$. Each data point represents the average of measurements for several different values of $H_z$.

It is clear from inspection of Fig. 3 that the detected bead field decreases as the arm width of the Hall sensor increases (low values of $a/w$ in Fig. 3). This is expected because the Hall voltage is proportional to the average magnetic field over the sensor area. It follows that efficient bead detection requires values of $a/w$ larger than 1, and Fig. 3 graphically demonstrates that detection of nanometer scale magnetic labels will require sensors that are fabricated with comparable minimum feature size.

Taking the limit $w\to 0$ and $z\to a$ in Eq. (2) gives the expectation $\langle B_z\rangle\to 2H_z$. Fits to the data in Fig. 3 do not approach this limit mainly due to either a separation $t$ between the bead and the Hall sensor, or to a reduction in magnetic moment of the bead. Bulk measurements on dilute ensembles of beads suggest it is not the latter. The two curves are fits to Eq. (2) using optimized values of $t=0.2$ $\mu$m for the 1.6 and 2.1 $\mu$m beads. Allowing for the known passivation thickness, this suggests an additional separation of about 90 nm between the surface of the bead and that of the Hall sensor. Using an effective sensing area of $2w^2$ would reduce this separation to about 60 nm.

Finally, another measurement is used to verify the dipolar nature of the field from an individual bead. A bead is centered over the Hall sensor and then lifted vertically a distance $l$ (up to $l=3.0$ $\mu$m) above the sensor surface. Figure

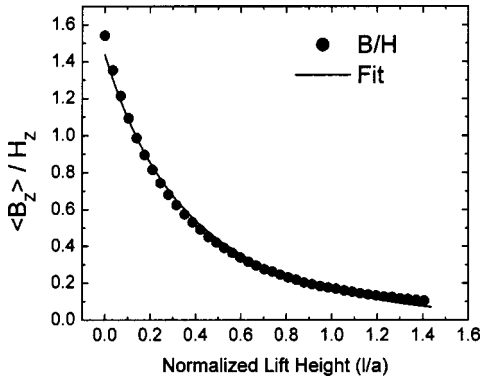


FIG. 4. Measured field for a 2.1 $\mu$m bead lifted from the surface of a 0.6 $\mu$m Hall cross. Solid curve is a fit to Eq. (2).

4 shows data from this experiment for a 2.1 $\mu$m bead lifted from the surface of a $w=0.6$ $\mu$m Hall sensor. The data are fit to Eq. (2) using the value of $t$ that was optimized in the fits of Fig. 3 and a moment $m=Ha^3$. The fit shown in Fig. 4 has no free parameter and the quality of the fit confirms that the field from the bead is almost purely dipolar.

In summary, we have characterized the magnetic properties of single micron-sized ferromagnetic particles using Hall sensors with minimum feature sizes from 500 nm to 2.5 $\mu$m. The particles we have measured exhibit a linear magnetization curve at low fields, and have a purely dipolar magnetic moment. We have demonstrated the geometrical scaling of the average field with sensor size and have shown that the optimal sensor sensitivity is achieved for sensors whose lateral dimension is smaller than the bead radius.

This work was performed while G.L. held a National Research Council Research Associateship Award at the Naval Research Laboratory. M.J. acknowledges support by ONR and DARPA BioMagnetICs. V.S. acknowledges the Faculty Research Grant at Towson University. The authors acknowledge Sommy Bounnak for her help with Hall sensor fabrication.

[1]D. R. Baselt, G. U. Lee, M. Natesan, S. W. Metzger, P. E. Sheehan, and R. J. Colton, Biosens. Bioelectron. **13**, 731 (1998).
[2]M. M. Miller, C. A. Prinz, S.-F. Cheng, and S. Bounnak, Appl. Phys. Lett. **81**, 2211 (2002).
[3]J. C. Rife, M. M. Miller, P. E. Sheehan, C. R. Tamanaha, M. Tondra, and L. J. Whitman, Sens. Actuators, A **107**, 209 (2003).
[4]P.-A. Besse, G. Boero, M. Demierre, V. Pott, and R. Popovic, Appl. Phys. Lett. **80**, 4199 (2002).
[5]C. Nguyen, B. Brar, H. Kroemer, and J. H. English, Appl. Phys. Lett. **60**, 1854 (1992).
[6]B. R. Bennett, B. P. Tinkham, J. B. Boos, M. D. Lange, and R. Tsai, J. Vac. Sci. Technol. B **22**, 688 (2004).
[7]S. Calvin, M. Miller, R. Goswami, S.-F. Cheng, S. Mulvaney, L. Whitman, and V. Harris, J. Appl. Phys. **94**, 778 (2003).
[8]I. S. Ibrahim, V. A. Schweigert, and F. M. Peeters, Phys. Rev. B **57**, 15416 (1998).
[9]M. Miller, P. Sheehan, R. Edeistein, C. Tamanaha, L. Zhong, S. Bounnak, L. Whitman, and R. Colton, J. Magn. Magn. Mater. **225**, 138 (2001).